# New experimental bremsstrahlung cross-section for light ion beams up to 60 MeV and comparison to theoretical models

F. Ralite, Charbel Koumeir, Arnaud Guertin, Ferid Haddad, Quentin Mouchard, Noël Servagent, Vincent Métivier

# NEW EXPERIMENTAL BREMSSTRAHLUNG CROSS-SECTION FOR LIGHT ION BEAMS UP TO 60 MeV AND COMPARISON TO THEORETICAL MODELS

Flavien Ralite[(1,3,*)], Charbel Koumeir[(2)], Arnaud Guertin[(1)], Ferid Haddad[(1,2)], Quentin Mouchard[(1)], Noel Servagent[(1)], and Vincent Metivier[(1)]

[(1)] Laboratoire SUBATECH, IMT Atlantique, CNRS/IN2P3, Nantes Université, Nantes, France

[(2)] GIP ARRONAX, Saint-Herblain, France

[(3)] Institut Bergonié, Bordeaux, France

*Corresponding author: f.ralite@bordeaux.unicancer.fr,

**ABSTRACT : Recent works focused on bremsstrahlung radiation as a non-invasive tool for monitoring proton beams used in radiobiology (>20 MeV). In order to study the validity of theoretical models of bremsstrahlung cross sections, bremsstrahlung X-rays between 4 keV and 15 keV coming from a carbon target irradiated by proton beams in the energy range from 15 MeV to 50 MeV were measured by a silicon drift detector. The obtained data vary from 10 mbarn.keV$^{-1}$ to 1000 mbarn.keV$^{-1}$ and fit well the literature and with theoretical model calculation. These results strongly support that bremsstrahlung X-rays models can be used to develop promising online tools for proton beam monitoring.**

**Keywords : Bremsstrahlung X-rays, Cross-Section, light ion beam, Carbon target**

## INTRODUCTION

The irradiation of a target with an ion beam produces X-rays by ionisation and bremsstrahlung, the latter being of continuous nature and often qualified as background radiation. Research teams working on Particle Induced X-ray Emission (PIXE) analysis are interested to model bremsstrahlung X-rays to improve their data by keeping only the characteristic X-rays emissions and removing the continuous background (Ishii, 2006a). This led to theoretical studies on bremsstrahlung cross-section models for proton beams in the energy range 2-20 MeV (Ishii, 2006a; Ishii and Hitomi, 2018).

Recently, bremsstrahlung X-rays have attracted interest in the fields of hadrontherapy and radiobiology. Some studies dealing with the bremsstrahlung radiations as a non-invasive tool to monitor the proton beam range from 20 MeV up to 230 MeV have been conduced (Yamaguchi et al., 2016a, 2016b, 2012). In this context, we have investigated the use of Bremsstrahlung X-rays emitted by a low Z millimeter thick medium for the on-line control of ion beams (Koumeir et al., 2019; Schwob et al., 2015) for radiobiology experiments performed with the ARRONAX cyclotron (located in Saint-Herblain, France (Haddad et al., 2008)).

The aim of this paper is to evaluate the validity of the theoretical model of the bremsstrahlung cross-section, developed for PIXE experiments, for proton and alpha beams in the energy range available with the ARRONAX cyclotron. Therefore, this work presents cross-section measurements of bremsstrahlung X-rays coming from a carbon target irradiated with proton beams ranging from 15 MeV up to 50 MeV and alpha particles at a fixed energy of 62 MeV. Carbon was chosen because it is a light element close to the atomic number of the water (reference medium in radiobiology experiments), as well as the thickness of the carbon sheet can be accurately determined for cross-section measurement and it is easy to handle. The experimental data measured during this work are compared with simulations based on theoretical works dealing with the bremsstrahlung cross-

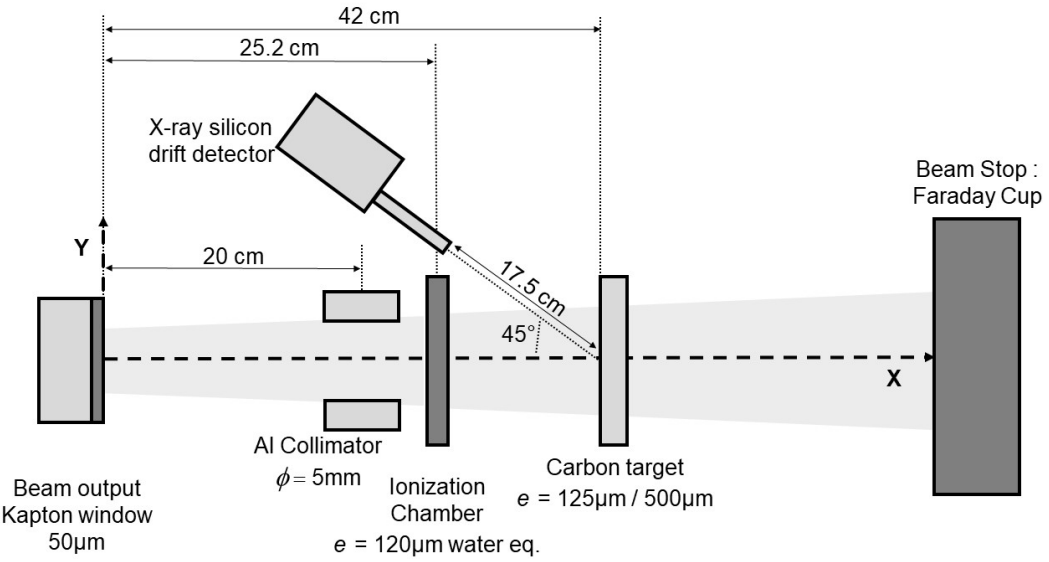


Figure 1. Illustration of the experimental set-up.

sections (Chu et al., 1981; Ishii, 2006a, 1995; Miraglia, 1989; Pacher and Miraglia, 1990).

## MATERIALS AND METHODS

### Simulation of the bremsstrahlung cross section

The deceleration of a charged particle moving in a medium produces bremsstrahlung radiations. The energy $h\nu$ of the created photon is proportional to the energy loss of the charged particle. These radiations constitute the continuous component presents in all experimental X-ray spectra.

It's usual to identify four different processes in the bremsstrahlung emission induced by ion irradiation, called: Quasi-Free-Electron Bremsstrahlung (QFEB), Secondary Electron Bremsstrahlung (SEB), Atomic Bremsstrahlung (AB) and, Nuclear Bremsstrahlung (NB) (Amusia, 2006; Chu et al., 1981; Ishii, 2006a, 1995; Miraglia, 1989; Pacher and Miraglia, 1990). The NB will not be included in our simulation for this study. As its signal is inversely proportional to the square of the projectile mass and the square of its velocity, its contribution is very negligible, compared to the other components of the bremsstrahlung, for a proton beam in the energy range of several tens of MeV. Ishii's paper (Ishii, 2006a) describes all of these components, which have maximum energies such as $h\nu_{max}^{QFEB} < h\nu_{max}^{SEB} < h\nu_{max}^{AB}$:

$$h\nu_{max}^{QFEB} = \frac{m_e}{m_p} E_p \quad (1)$$

$$h\nu_{max}^{SEB} = 4\frac{m_e}{m_p} E_p \quad (2)$$

$$h\nu_{max}^{AB} \propto \frac{Z_T}{\left(\frac{Z_p Z_T m_e}{m_p}\left(1-\frac{m_p Z_T}{m_T Z_p}\right)\right)^{1/4}} \quad (3)$$

Where $\frac{m_e}{m_p}$ is the ratio of the electron mass at rest and the projectile mass at rest, $E_p$ is the beam energy, $m_T$ is the mass at rest of the target. $Z_p$ and $Z_T$ are respectively the atomic numbers of the projectile and the target (Ishii, 2006a).

The total differential cross-section of the Bremsstrahlung X-rays $\frac{d^2\sigma^{Br}}{d\Omega dh\nu}$ is the sum of QFEB, SEB, and AB cross-sections, as mentioned below.

$$\frac{d^2\sigma^{Br}}{d\Omega dh\nu}\left(E_p, h\nu, \theta\right) = \frac{d^2\sigma^{QFEB}}{d\Omega dh\nu} + \frac{d^2\sigma^{SEB}}{d\Omega dh\nu} + \frac{d^2\sigma^{AB}}{d\Omega dh\nu} \quad (4)$$

The cross-sections of each bremsstrahlung component, i, can be expressed as the product of two factors called strength $F_{1i}$ and shape $F_{2i}$ factors. The strength factor depends on $E_p$, $Z_p$, and $Z_T$ whereas the shape factor depends on the X-ray emission angle $\theta$.

$$\frac{d^2\sigma^{i}}{d\Omega dh\nu} = F_{1i}\left(E_p, Z_p, Z_T\right) \cdot F_{2i}\left(\theta\right) \quad (5)$$

In this study, a homemade python program, based on the theoretical bremsstrahlung cross-

sections, simulates the bremsstrahlung spectra. The models of *Ishii et al* (Ishii, 2006a, 1995), *Miraglia et al* (Miraglia, 1989), *Pacher et al.* (Pacher and Miraglia, 1990) and *Chu et al.* (Chu et al., 1981) were used to determine the differential cross-sections.

## Measurement of the Bremsstrahlung X-rays

### *Experimental set-up*

The ARRONAX cyclotron (IBA C70) delivers alpha and proton beams through a 50 µm thick Kapton exit window (Figure 1). The energy of alpha beam at the target position was 62 MeV, and the energy of proton beams at this position were 15 MeV, 29 MeV, 32 MeV, 39 MeV, and 49 MeV. A collimator placed 20cm after the beam output window narrowed the beam on the carbon target. Carbon target thicknesses were 125 µm for alpha (62 MeV) and proton beam (15 MeV, 29 MeV, 39 MeV), and 500 µm for the 49 MeV energy proton beam. The foils, supplied by the GoodFellow Company, have 25×25 $mm^2$ surface and are of high purity (99.9%). The exit window-target distance was 42 cm. Photon detection was performed using a silicon drift detector (SDD) positioned at an angle of 45° between the detector axis and the incident beam direction. The target-detector distance was 17.5 cm.

### *Beam intensity monitoring*

The equation (6) links the number of incident charged particles $N_p$ to the beam fluence $Q$ by:

$$N_p = \frac{Q}{Z_p \cdot e} \quad (6)$$

An ionisation chamber, placed in front of the target and calibrated with an instrumented Faraday cup for different beam energies, measured the beam fluence. The calibration was done with the same experimental set-up but without the target. The uncertainty on the measured beam fluence was about 1.5%, and came from electronic acquisition device and the standard deviation of the ion chamber response. The temperature and pression in the experimental room did not change during the measurements. The calibration of the ionisation chamber was checked before and after each beam energy measurement.

## Cross-Section Measurement

For each channel of the SDD spectrum, a background removal cleans the experimental data of undesirable statistical events. The background spectra were measured without the target inside the experimental set-up. Each spectrum (background and bremsstrahlung) was normalised with the beam fluence, measured by the ionisation chamber, before subtracting the background spectrum to the bremsstrahlung spectrum. The cross-section determination considers the correction of the detector efficiency and the medium attenuation as indicated in the equation (7):

$$\frac{d\sigma}{dh\nu} = \frac{1}{dh\nu} \sum_{i=1}^{N} \frac{N_i^{XR} \cdot M_C}{N_p \cdot \varepsilon_i \cdot \mathcal{A}_i \cdot \mathcal{N}_a} \quad (7)$$

Where $\sigma$ is the bremsstrahlung cross section at the photon energy $h\nu$ ; $N_i^{XR}$, $\varepsilon_i$ and $\mathcal{A}_i$ are respectively the number of measured X-rays, the detector efficiency, and the medium attenuation for the $i^{th}$ photon energy $h\nu$ ; N is the total number of channels of the SDD spectrum, each one corresponds to photon energy i ; $M_C$ is the molar mass of the carbon target and $\mathcal{N}_a$ is the Avogadro constant. The cross-sections are calculated for the mean energy photon centred on an energy window $dh\nu$. The latter (0.4 keV) was determined to get significant statistical counts (1000 counts minimum) and to satisfy a cross section variation below 5%.

The medium attenuation was determined using the X-mass attenuation database (Hubbell and Seltzer, 2004) and knowing the real thicknesses ($e_{carbon}$) of the targets used. The measures of the surface ($s_{carbon}$) and the mass ($m_{carbon}$) of the carbon targets give the real thicknesses (equation (8)) with an uncertainty of 1.7% if one considers that the target is homogeneous.

$$e_{carbon} = \frac{m_{carbon}}{s_{carbon} \cdot \rho_{carbon}} \quad (8)$$

Where $\rho_{carbon}$ is the carbon density equal to 2.25 $g/cm^3$.

The detection efficiency $\varepsilon_i$ was estimated using the Mohanty *et al* (Mohanty et al., 2008) model for each bin, i, of the X-ray spectrum. The Nelson Bachmann formula takes into account the fractional solid angle (Mohanty et al., 2008). The model was validated experimentally with a deviation of less than 3%thanks to calibrated

radioactive sources ($^{109}$Cd and $^{55}$Fe) as shown in figure 2.

The error associated to the cross-section measurement contains the errors on the incoming particles number, the detector efficiency, the target thickness and the uncertainty on the number of X-rays.

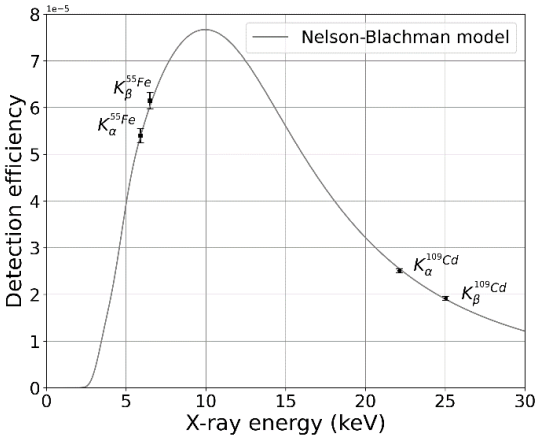


Figure 2. The normalised detection efficiency of the silicon drift detector modelled with the Nelson-Blachman formula (Mohanty et al., 2008). The model was experimentally checked with calibrated radioactive sources of $^{55}$Fe and $^{109}$Cd.

## RESULTS & DISCUSSION

### *Bremsstrahlung spectra from carbon target*

Figure 3 presents X-rays raw spectra from the carbon target (125 µm thick) and the background (obtained in the same experimental conditions but using a blank target) for a proton beam of 39 MeV. The characteristic X-ray peak of argon (2.9 keV), coming from the beam/air interaction, appeared clearly in both spectra. During the irradiation, the beam interacts with the different components of the experimental set-up and creates gamma radiations which can interact with the SDD detector and generate Compton radiations. These last participate in the continuous part of the X-ray spectra measured with and without the target. The difference between both spectra (figure 3) mainly comes from the bremsstrahlung signal and the Compton radiations generated by the gamma rays produced in the target. The shape of the bremsstrahlung spectrum is dependent on the SDD efficiency which promotes the detection of the X-rays between 2 keV and 13 keV as shown in figure 2.

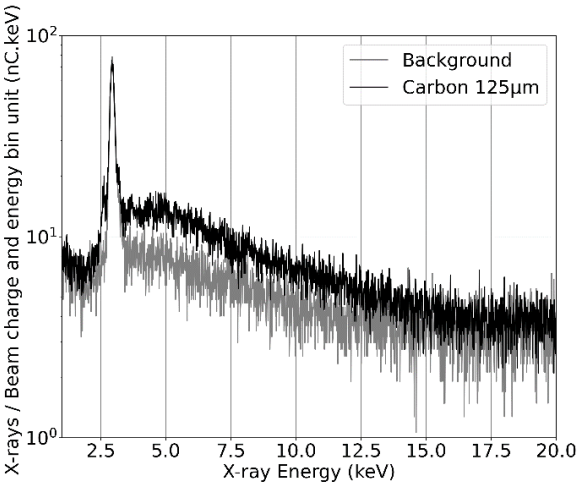


Figure 3. X-rays spectra from background and carbon with 39 MeV proton beam.

Figure 4 shows the bremsstrahlung spectra coming from the interaction between the carbon target and protons of 15 MeV and 49 MeV. Background spectra were subtracted from the target spectra. Lines correspond to our simulation results based on the theoretical cross section (Ishii, 2006b; Miraglia, 1989; Pacher and Miraglia, 1990). In both cases, they reproduce the experimental spectra quite well when taking into account the detection efficiency of the detector and the medium/air attenuation of the X-rays. The steep drop of the simulation curves signs the energy limit of the QFEB ($h\nu_{max}^{QFEB}$). In this study, the model considers the electrons of the target at rest, explaining the shape of the QFEB fall-off. By taking into account the velocity of the electron of the target, the QFEB fall-off should be smoother (Chu et al., 1981). Above the maximum energy of QFEB, only the SEB contributes to the bremsstrahlung spectra (AB has a negligible contribution compared to the two previous mechanisms), decreasing the bremsstrahlung radiations detected ahead of the Compton radiations produced in the target. The latter explains the discrepancies with the simulation in the high energy X-ray domain. $h\nu_{max}^{QFEB}$ depends on the beam energy as mentioned by equation (1), explaining the difference between spectra of 15 and 49 MeV.

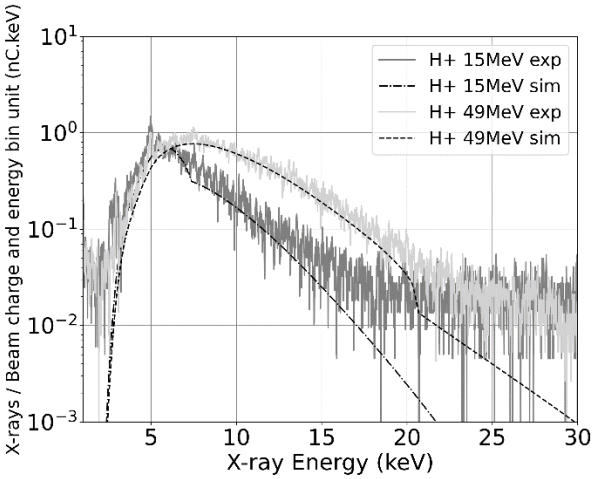


Figure 4. Bremsstrahlung spectra coming from the interaction between the carbon target and protons of 15 MeV and 49 MeV. Grey solid lines present the measurements whereas black dashed lines correspond to the simulation.

### *Bremsstrahlung cross sections*

Figure 5 shows the measured and simulated differential cross-section of 20 MeV (Ishii and Hitomi, 2018) and 15 MeV protons (this work) on a carbon target. The underestimation of the model, for X-rays above 12 keV, comes from the Compton background component induced by the target as mentioned in Ishii's paper (Ishii and Hitomi, 2018) as the theoretical model does not consider the Compton scattering in the target. As expected, the results presented in Ishii's study are quite close to the bremsstrahlung cross sections measured in this work, because the two beams have close energy.

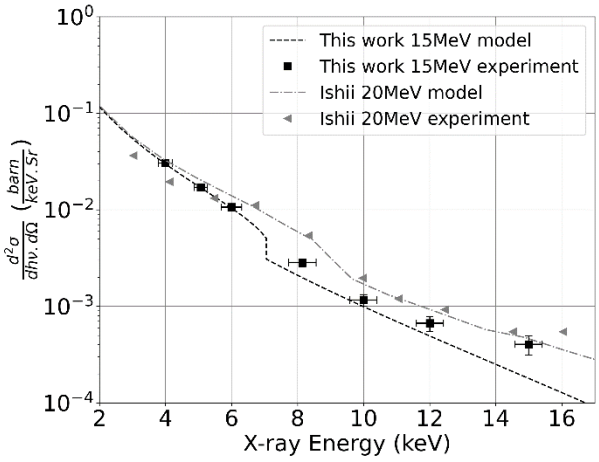


Figure 5. Comparison of the differential cross sections of the bremsstrahlung X-rays coming from a carbon target irradiated with proton beams of 15 MeV (this study) and 20 MeV (Ishii's study). The dotted line corresponds to theoretical values.

Figure 6 shows the simulated and measured differential bremsstrahlung cross sections for alpha particle and proton beams with different energies. The magnitude of the differential measured cross-section is from 10 mbarn.keV$^{-1}$ to 1000 mbarn.keV$^{-1}$. Therefore, the Bremsstrahlung X-rays signals generated by a light medium (millimetric thickness) could be significant for online beam monitoring applications in the ARRONAX energy range (17.5 MeV to 70 MeV for protons and 70 MeV for alpha particles (Haddad et al., 2008)). For the 15 MeV and 49 MeV proton beams, an additional experiment reproduced the data with a deviation under 3 % included in the error bar. The model fits the experimental data for the photon energies lower than the QFEB limits. Simulations slightly underestimated the experiment for higher photon energies because of the increasing of the Compton background produced by the target relatively to the SEB bremsstrahlung signal.

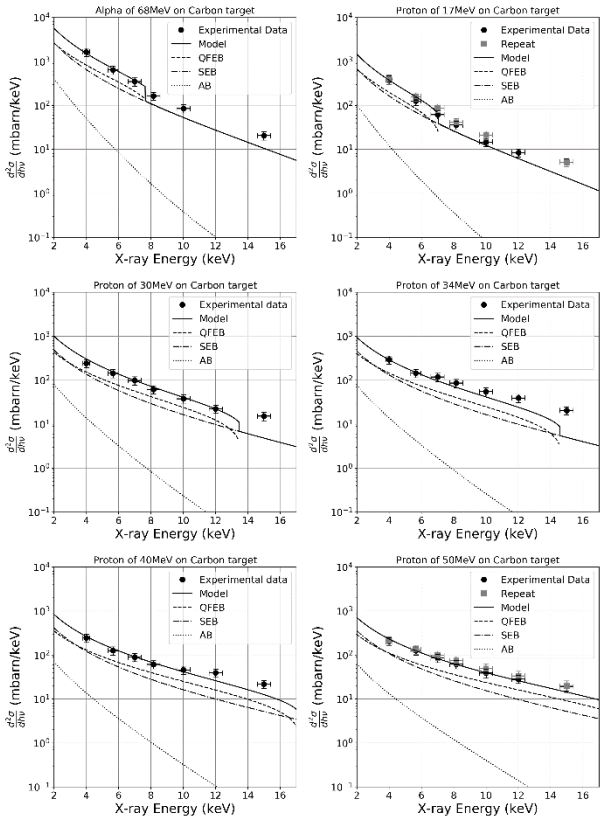


Figure 6. Bremsstrahlung cross sections for a carbon target bombarded with alpha of 62 MeV and protons of 15 MeV, 29 MeV, 33 MeV, 39 MeV, and 49 MeV. Experimental data (point marker) with their respective simulations are presented: Total bremsstrahlung (solid line), and the bremsstrahlung components QFEB (dashed line), SEB (point-dashed line) and AB (point line).

Apart the high energy X-rays region, the good agreement between the experimental and theoretical data validates the bremsstrahlung model for the proton beam in the energy range from 15 MeV to 50 MeV. Similar agreement is obtained with the alpha beam of 62 MeV. Further experiments are necessary to improve the cross-section measurement for X-rays bremsstrahlung above the QFEB limit, an active shielding (Hurtado et al., 2006; Pointurier et al., 1996) to reject the Compton radiations created by the interaction of the gamma-ray with the target. Also, the model used to simulate the bremsstrahlung spectra can include the background part by considering the nuclear reaction phenomenon. In addition, measurements using a detector with better efficiency at higher X-ray energies are needed to check the validity of the model for hadrontherapy applications.

## CONCLUSION

This study presents a comparison of measured and simulated Bremsstrahlung cross-section based on theoretical models in an extended energy range for protons (up to 50 MeV) and for alpha beam (62 MeV).

Results for alpha (62 MeV) and proton beams (15 MeV - 49 MeV) show a significant production of the bremsstrahlung X-rays (from 10 to 1000 mbarn. $keV^{-1}$). This confirms that bremsstrahlung X-rays can be a tool to monitor light ion beams.

Experimental measurements for 15 MeV the proton beam are closed to those of Ishii's work (Ishii and Hitomi, 2018) performed at 20 MeV. The agreement of the simulated bremsstrahlung cross-sections with the experimental data shows the model consistency in the ARRONAX energy range. However, the model underestimates the number of high energy X-rays, for which Compton radiation produced in the target starts to compete with bremsstrahlung radiations.

These results are promising for the possible use of bremsstrahlung X-rays as an online tool for proton beam monitoring even if further investigations are required to extend the energy range under consideration with an appropriate X-ray detector. The latter takes part in a challenge in radiobiology and hadrontherapy applications.

## ACKNOWLEGMENTS

The authors thank the accelerator group and risk management group of the ARRONAX Public Interest Group (GIP). This project is partially supported by grants from the French National Agency for Research called "Investissements d'Avenir", Equipex Arronax-Plus (ANR-11-EQPX-0004), Labex IRON (ANR-11-LABX-18-01), and ISITE NExT (ANR-16-IDEX-0007).

## REFERENCES

Amusia, M.Ya., 2006. "Atomic Bremsstrahlung": Retrospectives, current status and perspectives. Radiation Physics and Chemistry 75, 1232–1250. https://doi.org/10.1016/j.radphyschem.2006.04.009

Chu, T.C., Ishii, K., Yamadera, A., Sebata, M., Morita, S., 1981. Quasifree electron bremsstrahlung induced by 20-MeV-proton impact. Phys. Rev. A 24, 1720–1725. https://doi.org/10.1103/PhysRevA.24.1720

Haddad, F., Ferrer, L., Guertin, A., Carlier, T., Michel, N., Barbet, J., Chatal, J.-F., 2008. ARRONAX, a high-energy and high-intensity cyclotron for nuclear medicine. Eur J Nucl Med Mol Imaging 35, 1377–1387. https://doi.org/10.1007/s00259-008-0802-5

Hubbell, J.H., Seltzer, S.M., 2004. X-Ray Mass Attenuation Coefficients. NIST Standard Reference Database 126. https://dx.doi.org/10.18434/T4D01F

Hurtado, S., García-León, M., García-Tenorio, R., 2006. Optimized background reduction in low-level gamma-ray spectrometry at a surface laboratory. Applied Radiation and Isotopes 64, 1006–1012. https://doi.org/10.1016/j.apradiso.2006.01.008

Ishii, K., 2006a. Continuous X-rays produced in light-ion–atom collisions. Radiation Physics and Chemistry 75, 1135–1163. https://doi.org/10.1016/j.radphyschem.2006.04.008

Ishii, K., 2006b. Continuous X-rays produced in light-ion–atom collisions. Radiation Physics and Chemistry 75, 1135–1163. https://doi.org/10.1016/j.radphyschem.2006.04.008

Ishii, K., 1995. High energy limit of atomic bremsstrahlung. Nuclear Instruments and Methods in Physics Research Section B: Beam Interactions with Materials and Atoms 99, 163–165. https://doi.org/10.1016/0168-583X(94)00571-0

Ishii, K., Hitomi, K., 2018. Theoretical detection limit of PIXE analysis using 20 MeV proton beams. Nuclear Instruments and Methods in Physics Research Section B: Beam Interactions with Materials and Atoms 417, 37–40. https://doi.org/10.1016/j.nimb.2017.10.008

Koumeir, C., De Nadal, V., Cherubini, R., Cherel, M., Garrido, E., Gouard, S., Guertin, A., Haddad, F., Metivier, V., Michel, N., Poirier, F., Servagent, N., Soulanet, T., Varmenot, N., 2019. The radiobiological platerform at at ARRONAX. Radiat Prot Dosimetry 183, 270–273. https://doi.org/10.1093/rpd/ncy301

Miraglia, J.E., 1989. Scaling laws for secondary-electron bremsstrahlung. Phys. Rev. A 39, 2908–2913. https://doi.org/10.1103/PhysRevA.39.2908

Mohanty, B.P., Balouria, P., Garg, M.L., Nandi, T.K., Mittal, V.K., Govil, I.M., 2008. Comparison of experimental and theoretical efficiency of HPGe X-ray detector. Nuclear Instruments and Methods in Physics Research Section A: Accelerators, Spectrometers, Detectors and Associated Equipment 584, 186–190. https://doi.org/10.1016/j.nima.2007.10.017

Pacher, M.C., Miraglia, J.E., 1990. Scaling laws and polarization of atomic and nuclear bremsstrahlung. Phys. Rev. A 41, 2574–2579. https://doi.org/10.1103/PhysRevA.41.2574

Pointurier, F., Laurec, J., Blanchard, X., Adam, A., 1996. Cosmic-ray induced background reduction by means of an anticoincidence shield. Applied Radiation and Isotopes 47, 1043–1048. https://doi.org/10.1016/S0969-8043(96)00103-0

Schwob, L., Koumeir, C., Servagent, N., Cherel, M., Guertin, A., Haddad, F., Métivier, V., Michel, N., Poirier, F., Rahmani, A., Varmenot, N., 2015. New beam monitoring tool for radiobiology experiments at the cyclotron ARRONAX. Radiat Prot Dosimetry 166, 257–260. https://doi.org/10.1093/rpd/ncv199

Yamaguchi, M., Nagao, Y., Ando, K., Yamamoto, S., Toshito, T., Kataoka, J., Kawachi, N., 2016a. Secondary-electron-bremsstrahlung imaging for proton therapy. Nuclear Instruments and Methods in Physics Research Section A: Accelerators, Spectrometers, Detectors and Associated Equipment 833, 199–207. https://doi.org/10.1016/j.nima.2016.07.034

Yamaguchi, M., Torikai, K., Kawachi, N., Shimada, H., Satoh, T., Nagao, Y., Fujimaki, S., Kokubun, M., Watanabe, S., Takahashi, T., Arakawa, K., Kamiya, T., Nakano, T., 2016b. Corrigendum: Beam range estimation by measuring bremsstrahlung (2012 *Phys. Med. Biol* . **57** 2843). Phys. Med. Biol. 61, 3638–3644. https://doi.org/10.1088/0031-9155/61/9/3638

Yamaguchi, M., Torikai, K., Kawachi, N., Shimada, H., Satoh, T., Nagao, Y., Fujimaki, S., Kokubun, M., Watanabe, S., Takahashi, T., Arakawa, K., Kamiya, T., Nakano, T., 2012. Beam range estimation by measuring bremsstrahlung. Phys. Med. Biol. 57, 2843–2856. https://doi.org/10.1088/0031-9155/57/10/2843